OPEN

Original Article

PIM1 is a Poor Prognostic Factor for and Potential Therapeutic Target in Serous Carcinoma of the Endometrium

Hodaka Takeuchi, M.D., Tsutomu Miyamoto, M.D., Ph.D., Chiho Fuseya, M.D., Ph.D., Ryoichi Asaka, M.D., Ph.D., Koichi Ida, M.D., Ph.D., Motoki Ono, M.D., Yasuhiro Tanaka, M.D., Manaka Shinagawa, M.D., Hirofumi Ando, M.D., Ph.D., Shiho Asaka, M.D., Ph.D., and Tanri Shiozawa, M.D., Ph.D.

Summary: Serous carcinoma (SC) is an aggressive histologic type of endometrial carcinoma (EMC) with a poor prognosis. The development of novel therapeutics for SC is an important issue. PIM1 is a serine/threonine kinase involved in various cellular functions, such as cell cycle progression, apoptosis, and transcriptional activation via the phosphorylation of many target proteins, including MYC. PIM1 is overexpressed in several cancers and has been associated with the treatment-resistance. We investigated the expression and function of PIM1 in EMC, particularly SC. Immunohistochemical analysis in 133 EMC cases [103 endometrioid carcinomas (EC) and 30 SC] revealed the significantly stronger expression of PIM1 in SC than in EC and significantly shorter survival of patients with the overexpression of PIM1 in all EMC cases, as well as in only SC cases. A multivariate analysis identified the overexpression of PIM1 as an independent prognostic factor. The knockdown of PIM1 by siRNA in the SC cell line, ARK1, decreased the expression of phosphorylated MYC and reduced proliferation, migration, and invasion. The PIM1 inhibitor, SGI-1776, reduced cell viability in SC cell lines (ARK1, ARK2, and SPAC1L) with IC50 between 1 and 5 μM. SGI-1776 also reduced the migration and invasion of ARK1 cells. Moreover, the oral administration of SGI-1776 significantly suppressed subcutaneous ARK1 xenograft tumor growth in nude mice without impairing health. These results indicate that PIM1 is involved in the acquisition of aggressiveness and suggest the potential of PIM1 as a novel therapeutic target and SGI-1776 as a therapeutic agent for SC. **Key Words:** PIM1—SGI-1776—Uterine serous carcinoma—Endometrial carcinoma—MYC.

The corpus uteri is the second common cancer site among gynecologic organs, with 417,367 newly diagnosed cases worldwide in 2020 according to the Global Cancer Observatory (https://gco.iarc.fr/) public data. Most cancers in the corpus uteri are endometrial carcinoma (EMC). Endometrioid carcinoma (EC) is the most common histologic type of EMC, while serous carcinoma (SC) is less common, but more aggressive than EC (1). In recent years, there have been noteworthy developments in the treatment landscape of uterine SC (USC), including human epidermal growth factor receptor 2-targeted therapy, antiangiogenics, and, more recently, cell cycle modulators (2–5). However, the improvement of treatment outcomes in USC patients is not sufficient enough. Therefore, the search for new therapeutic targets is mandatory.

The signaling pathways that are essential for cell function, such as proliferation, survival, and migration, are activated by protein phosphorylation and inactivated by dephosphorylation. Therefore, protein kinases, such as RAS and RAF, that phosphorylate downstream proteins are often oncogenes, while protein phosphatase generally functions as a tumor suppressor gene (6).

The Pim-1 proto-oncogene (PIM1) is a serine/threonine protein kinase that phosphorylates multiple factors, including MYC (7) and BCL2 (8), and is involved in the regulation of critical processes, such as cell cycle progression, apoptosis, and transcriptional activation (9). PIM1 is a member of the PIM kinase family, which comprises 3 homologous proteins, PIM1, PIM2, and PIM3, and is regulated by the JAK/STAT pathway (10). The overexpression of PIM1 has been reported in several malignancies, such as leukemia, malignant melanoma, and prostate cancer, and has been associated with the development of treatment resistance in these cancers (11–14). Brasó-Maristany et al. (9) recently showed that the overexpression of PIM1 was frequently detected in triple-negative breast cancer and is critical for tumor growth. These findings prompted us to investigate the expression of PIM1 in EMC, particularly USC, because the Cancer Genome Atlas (TCGA) data showed a high correlation of genetic characterization between USC and triple-negative/basal-like breast cancers (15).

In the present study, we examined the expression and function of PIM1 in EMC. The results obtained revealed a correlation between the overexpression of PIM1 and a poor prognosis in EMC patients, particularly SC. PIM1 contributed to the proliferation of and invasion and migration by SC cells. These results indicated the important role of PIM1 in the acquisition of the malignant potential of EMC, particularly SC, suggesting its potential as a therapeutic target.

MATERIALS AND METHODS

Patients and Tissue Samples

We selected 133 patients with EMC, including 103 EC (62 grade 1, 21 grade 2, and 20 grade 3) and 30 SC, treated at Shinshu University Hospital between 1997 and 2017. Ten out of the 30 SC cases had adjacent serous endometrial intraepithelial carcinoma (EIC) lesions. Formalin-fixed paraffin-embedded tissue specimens were obtained from these patients by hysterectomy and subjected to immunohistochemistry (IHC). The clinical information of each patient, including survival data, was collected from the electronic medical record system. Two or more pathologists at the Division of Laboratory Medicine cooperated to pathologically diagnose each case according to the WHO classification. The present study was approved by the Ethics Committee of Shinshu University School of Medicine (approval number: 4142). The requirement for informed consent in the present study was waived because we already obtained comprehensive consent to use medical records for any retrospective research from patients and provided them with the opportunity to opt-out of this study.

IHC and Evaluation

We performed IHC as previously described (16). Briefly, indirect immunostaining for PIM1 and phosphorylated MYC was performed using anti-PIM1 (rabbit polyclonal, 1:100 dilution, Abcam, Cambridge, UK) and anti-phospho-c-Myc (Ser62, rabbit polyclonal, 1:100 dilution, Abcam), respectively, as primary antibodies. Histofine Simple Stain Max-PO (Nichirei Bioscience Inc., Tokyo, Japan) was used as the secondary antibody. Three-micrometer-thick sections were deparaffinized in Hemo-De (FALMA, Tokyo, Japan) and rehydrated in a graded alcohol series. Antigens were retrieved by a microwave pretreatment in 10 mM Tris/HCl buffer (pH 8.0) containing 1 mM EDTA for 30 min. Sections were then exposed to primary antibodies at room temperature for 60 min. As negative controls, tissue sections were treated with a buffered solution without the primary antibody. These sections were then incubated with the secondary antibody at room temperature for 30 min. The immunocomplex was visualized by diaminobenzidine.
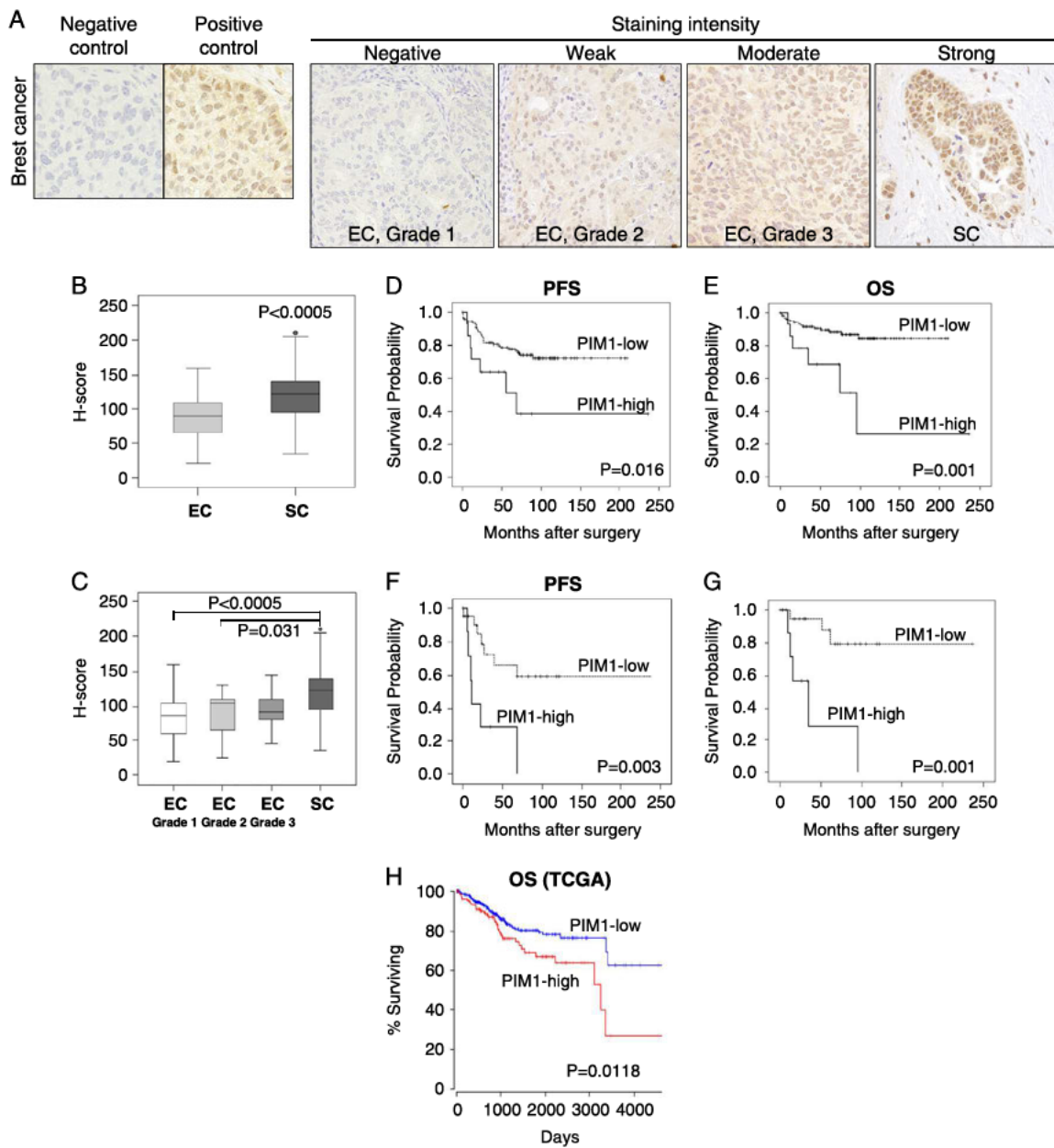
FIG. 1. Results of immunohistochemical staining for PIM1 in endometrial carcinoma (EMC). (A) Representative cases with negative (similar to a negative control), weak, moderate (similar to a positive control), and strong nuclear staining intensity. (B and C) PIM1 H-scores (maximum score = 300) were compared among histologic types. The H-score of serous carcinoma (SC) was significantly higher than that of endometrioid carcinomas (EC) ($P < 0.0005$) (B). Among EC cases, grades 1 and 2 were significantly lower than SC ($P < 0.0005$ in grade 1, $P = 0.031$ in grade 2), whereas grade 3 was not significantly different from SC (C). (D–G) Survival analysis by the Kaplan-Meier method. The progression-free survival (PFS) (D) and overall survival (OS) (E) of EMC patients with PIM1-high (H-score ≥ 140, over 90 percentile) were significantly shorter than those with PIM1-low (H-score < 140) ($P = 0.016$ in PFS, $P = 0.001$ in OS). The PFS (F) and OS (G) of SC patients with PIM1-high (H-score ≥ 141, higher than the 75th percentile) were significantly shorter than those with PIM1-low (H-score < 141) ($P = 0.003$ in PFS, $P = 0.001$ in OS). (H) Survival analysis based on the Cancer Genome Atlas (TCGA) data set of PIM1 gene expression in EMC patients. The OS of PIM1-high (higher than the 75th percentile) was significantly shorter than that of PIM1-low (less than the 75th percentile) ($P = 0.0118$).

TABLE 1. *Univariate and multivariate analyses of clinicopathologic factors influencing survival*

Parameters	N	PFS Uni P	OS Uni P	Multi 1* HR (95% CI)	Multi 1* P	Multi 2† HR (95% CI)	Multi 2† P
PIM1‡							
Low	119	0.616	**0.014**	**0.312 (0.117–0.833)**	**0.020**	0.361 (0.098–1.333)	0.126
High	14						
Age							
<70	110	0.588	0.221			0.768 (0.256–2.310)	0.639
≥70	23						
FIGO stage							
I-II	97	**0.005**	**<0.001**	**0.163 (0.065–0.412)**	**<0.001**	**0.167 (0.043–0.649)**	**0.010**
III-IV	36						
Histologic type							
EC	103	0.062	0.101			0.664 (0.154–2.864)	0.583
SC	30						
MI							
≤1/2	97	0.110	0.946			0.491 (0.135–1.781)	0.279
>1/2	36						
LVSI							
−	73	0.420	0.267			2.409 (0.728–7.980)	0.150
+	60						
LN metastasis							
−	103	0.698	0.205			0.934 (0.280–3.111)	0.911
+	30						

*Multi 1: multivariate analysis of significant factors identified in the univariate analysis.
†Multi 2: multivariate analysis of all factors.
‡PIM1 *H*-score ≥ 140 classified as high and <140 as low.
CI indicates confidence interval; FIGO, International Federation of Gynecology and Obstetrics; HR, hazard ratio; LN, lymph node; LVSI, lymphovascular space invasion; MI, myometrial invasion; Multi, multivariate analysis; OS, overall survival; PFS, progression-free survival; Uni, univariate analysis.

Immunoreactivity was evaluated by the Histo Score (*H*-score), which involved multiplying the staining intensity and stained percentage of 500 nuclei. The nuclear staining intensity was graded as follows: 0 = no stain (equal to the negative control), 1 = weak stain, 2 = moderate stain (equal to the positive control), 3 = strong stain. The *H*-score was calculated using the following formula: [1×(% nuclei of weak stain) + 2×(% nuclei of moderate stain) + 3×(% nuclei of strong stain)]. The final score ranged between 0 and 300.

Survival Analysis Using TCGA Data

We performed a survival analysis based on PIM1 mRNA expression levels using TCGA data at OncoLnc (http://www.oncolnc.org/), which contains survival and PIM1 mRNA expression data for 541 cases of uterine corpus endometrial carcinoma.

Cell Lines, PIM1 Knockdown (KD), and a PIM1 Inhibitor

The endometrial SC cell lines, ARK1, ARK2, SPAC-1L, and SPEC2 (17–19), were kindly provided by Prof. Baba at the Department of Obstetrics and Gynecology,

Iwate Medical University. These cell lines were cultured in RPMI 1640 medium (Sigma-Aldrich) with 10% FBS. Cells were incubated at 37°C in a 5% CO_2 incubator. PIM1-specific siRNA and scrambled siRNA (Control) (Origene, Rockville, MD) were used for PIM1-KD. According to the manufacturer's instructions, we used Lipofectamine MAX (Life Technologies, Carlsbad, CA) for siRNA transfection. PIM1-KD was confirmed by real-time RT-PCR and Western blotting. SGI-1776 (purchased from Selleckchem, S2198), which has high PIM1 selectivity among pan-PIM kinases, was used as the PIM1 inhibitor in experiments involving SC cells and mice.

Western Blotting

Protein expression levels in cultured cells were examined by Western blotting, as previously described (20). Anti-PIM1 (rabbit polyclonal, 1:1000 dilution, Cell Signaling Technology, Danvers, MA), anti-c-Myc (1:1000 dilution), anti-phospho c-MYC (1:1000 dilution), and anti-β-actin (mouse monoclonal, 1:2000 dilution, BioMakor, Rehovot, Israel) were used as the primary antibodies to detect PIM1, MYC, phospho-MYC, and β-actin, respectively. Protein-transferred
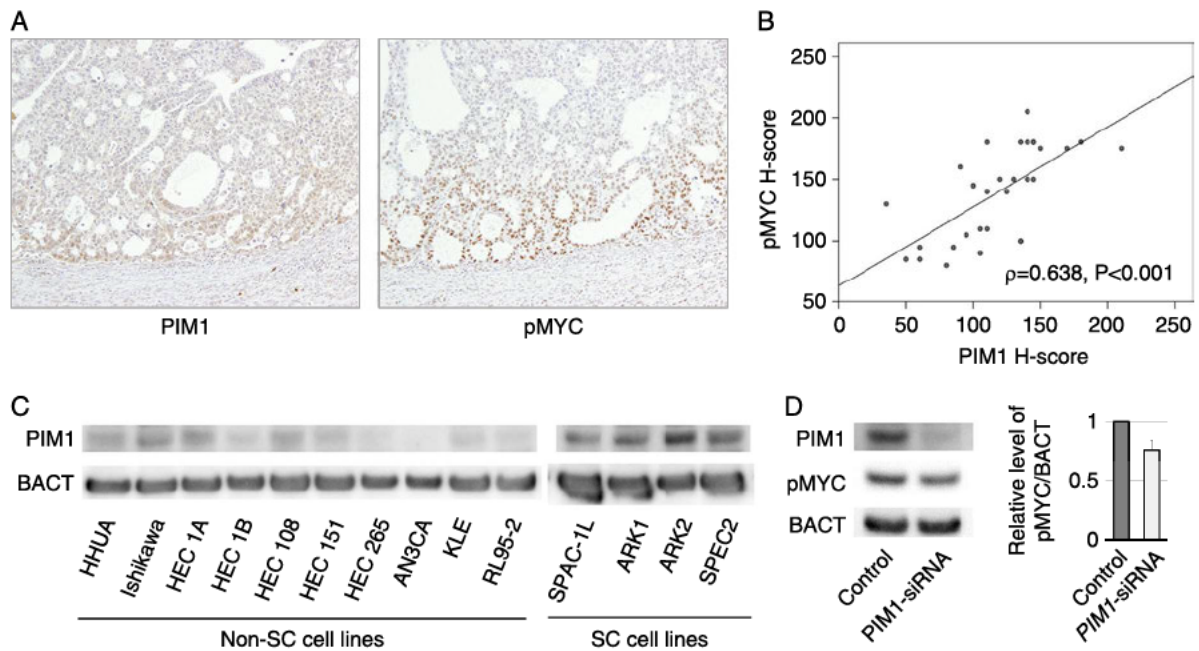
FIG. 2. (A) Immunohistochemical expression of PIM1 and phosphorylated MYC (pMYC). PIM1 and pMYC expression sites matched well. (B) Scatter plot of PIM1 and pMYC *H*-scores. The Spearman rank correlation coefficient revealed a strong correlation between both *H*-scores ($\rho = 0.638$, $P < 0.001$). (C) PIM1 protein expression in endometrial carcinoma (EMC) cell lines by Western blotting. PIM1 bands were stronger in serous carcinoma (SC) cell lines (ARK1, ARK2, SPAC1L, SPAC2) than in other EMC cell lines. Beta-actin (BACT) was used as the internal control. (D) PIM1-knockdown (KD) by PIM1-siRNA transfection in ARK1 cells. PIM1, pMYC, and BACT protein expression was examined by Western blotting. The graph indicates relative pMYC expression levels (mean and SD) corrected by BACT using densitometry in 3 experiments. PIM1 expression was weaker in PIM1-siRNA (PIM1-KD cells) than in the control transfected with scrambled siRNA. The expression of pMYC was also reduced in PIM1-siRNA.

membranes were incubated with the specific primary antibody at 4°C overnight and then with the secondary antibody at room temperature for 1 hr. The target protein band bound by the antibody complex was then visualized using the ECL Western blot detection reagent (Amersham, Piscataway, NJ).

Cell Proliferation/Viability Assay

The WST-1 assay was performed to analyze the proliferation or viability of SC cells under various conditions using WST-1 reagent (Roche Diagnostics, Basel, Switzerland) and a microplate reader (SYN-ERGY HT, Bio-Tek, Winooski, VT). As previously described (21), cells were seeded on a 96-well micro-plate at a density of 1000 cells/well. According to the manufacturer's instructions, the WST-1 assay was performed for 4 consecutive days after the confirma-tion of cell attachment to the bottom of wells.

Migration and Invasion Assays

We performed the transwell migration assay and Matrigel invasion assay to examine the migration and invasion abilities of SC cells, as previously described (22). According to the manufacturer's instructions, a transwell membrane (Corning BioCoat Control Insert without matrigel, Corning, New York, NY) was used for the transwell migration assay and a matrigel insert (Corning BioCoat Matrigel Invasion Chamber, Corn-ing) for the Matrigel invasion assay. Cells (1.0×10^5) in serum-free medium were placed into the upper chamber, medium with 10% FBS was added to the lower chamber as a chemoattractant, and cells were incubated at 37°C in a 5% CO_2 incubator. The incubation time for the migration assay was 8 hr, while the invasion assay was 20 hr. After cells remaining on the upper side of the membrane had been wiped off with a cotton swab, cells that migrated/invaded the membrane's underside were fixed and stained (Diff-Quick, Sysmex, Kobe, Japan) and then counted in 4 randomly selected microscopic fields.

In Vivo Experiments

Subcutaneous xenografts were established in the flanks of 6-wk-old female nude mice (BALB/c-nu, Charles River Laboratories Japan, Yokohama, Japan)

by an injection of 5×10^6 ARK1 cells. After confirming xenograft tumor formation with a diameter of ~5 mm, the oral administration of only solvent (control group) or SGI-1776 (SGI-1776 group, 75 mg/kg×5 times/wk) was initiated. Tumor volumes were calculated using the following approximate expression and indicated as a ratio to the tumor volume at the initiation of oral administration; tumor volume = 1/2×(long diameter)×(short diameter)^2. Mice were euthanized 3 wk after the initiation of oral administration. Subcutaneous xenograft tumors were then removed and their weights were measured. The Shinshu University Animal Experiment Committee approved the animal experiment (approval no. 300122), which was implemented in accordance with various animal experimental guidelines and regulations.

Statistical Analysis

We performed 2-group comparisons using the Mann-Whitney U test and multigroup comparisons of 3 or more groups using the Kruskal-Wallis test and Scheffé test. A correlation analysis was performed using Spearman rank correlation coefficient. A survival analysis was conducted using the Kaplan-Meier method. Univariate and multivariate analyses of prognostic factors were performed using Cox regression analysis. A P-value <0.05 was considered to be significant. These analyses were performed using SPSS version 24 (IBM, Armonk, NY).

RESULTS

Immunohistochemical Expression of PIM1 in EC

The expression of PIM1 was mainly detected in the nucleus (Fig. 1A). The H-score of the nuclear expression of PIM1 (median, 25th–75th percentile) was significantly higher in SC (122.5, 96.3–140.0) than in EC (90.0, 65.0–110.0) ($P<0.0005$) (Fig. 1B), particularly in comparisons with grade 1 EC (85.0, 65.0–103.8) ($P<0.001$) and grade 2 EC (105.0, 65.0–110.0) ($P=0.031$) (Fig. 1C). On the other hand, in 10 SC cases with adjacent EIC, the PIM1 H-score was significantly higher in SC (107.5, 70.0–132.5) than in EIC (55.0, 46.3–73.8) ($P=0.019$) (Supplementary Fig. 1, Supplemental Digital Content 1, http://links.lww.com/IJGP/A135). Among all EMC cases, PIM1-high (H-score ≥ 140, higher than the 90th percentile) showed significantly shorter progression-free survival (PFS) ($P=0.016$) (Fig. 1D) and overall survival ($P=0.001$) than PIM1-low (H-score <140, within the 90th percentile) (Fig. 1E). This prognostic difference was not

significant in EC cases (data not shown). However, in SC cases, PIM1-high (H-score ≥ 141, higher than the 75th percentile) showed significantly shorter PFS ($P=0.003$) (Fig. 1F) and overall survival ($P=0.001$) than PIM1-low (H-score <141, within the 75th percentile) (Fig. 1G). We performed univariate and multivariate Cox regression analyses of clinicopathologic factors potentially influencing survival, including PIM1 expression, age older than 70 yr, International Federation of Gynecology and Obstetrics (FIGO) stages III and IV, the histologic type, deep myometrial invasion, lymphovascular space invasion, and lymph node metastasis (Table 1). Among these factors, only the FIGO stage was identified as a significant poor prognostic factor for PFS ($P=0.005$). Although PIM1-high was not significant in the multivariate analysis of all factors, PIM1-high and FIGO advanced stages were both identified as significant poor prognostic factors in the multivariate analysis of the factors identified in the univariate analysis. The TCGA data set of EMC demonstrated that PIM1-high mRNA expression (higher than the 75th percentile) had significantly shorter overall survival than PIM1-low (within the 75th percentile) ($P=0.0118$) (Fig. 1H). These results suggest that the overexpression of PIM1 increased the malignant potential of EMC, particularly SC. Therefore, the function of PIM1 was examined in more detail using SC cell lines.

Expression of PIM1 and Phospho-MYC

Since MYC is a candidate of the PIM1 target protein for phosphorylation (7), we investigated the relationship between the expression of PIM1 and phospho-MYC. Immunohistochemical staining showed that the distribution of PIM1-overexpressing cells was consistent with that of phospho-MYC-positive cells (Fig. 2A). The Spearman rank correlation coefficient indicated that the H-score of PIM1 correlated with that of phospho-MYC ($\rho=0.638$, $P<0.001$) (Fig. 2B). We then examined the expression of PIM1 proteins in SC cell lines (SPAC1C, SPAC2, ARK1, and ARK2) and other EMC cell lines (Fig. 2C). Western blotting indicated the moderate to strong expression of PIM1 in all SC cell lines, and its weak expression in most of the other EMC cell lines. In ARK1, PIM1-KD by siRNA down-regulated the expression of phospho-MYC (Fig. 2D). These results suggest that MYC is a phosphorylated target of PIM1 in SC.

Effects of PIM1 Suppression on Cellular Functions in SC Cell Lines

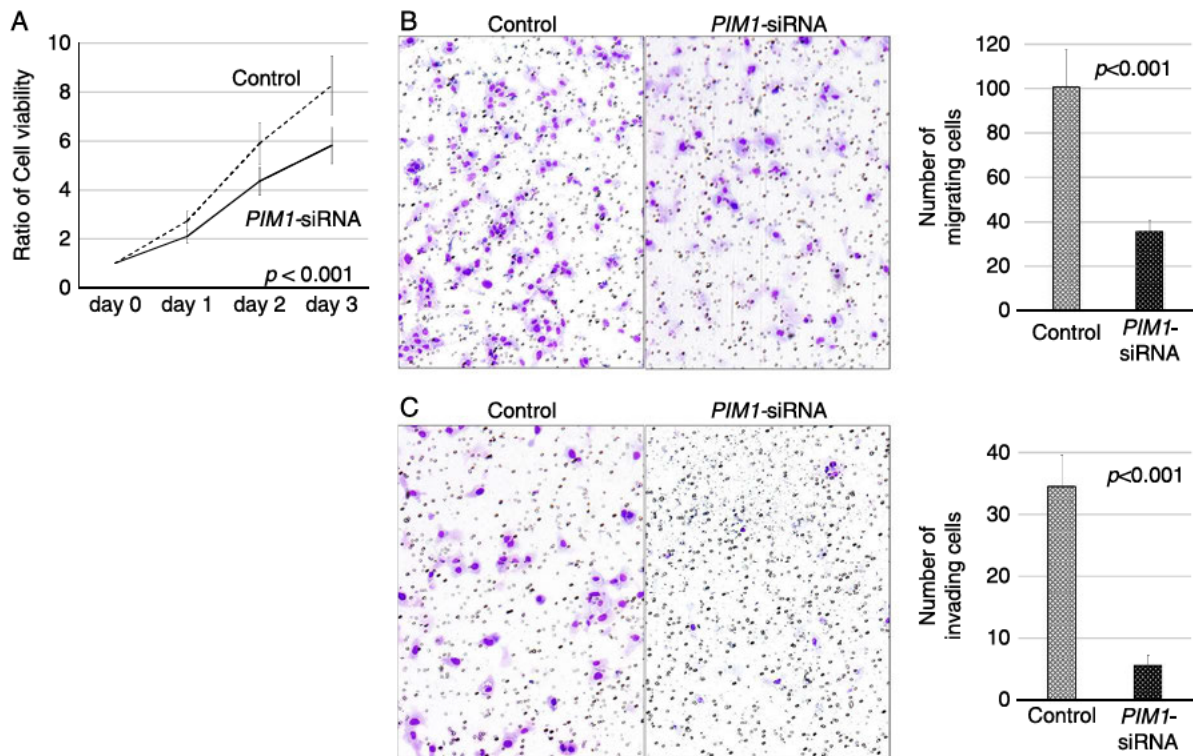We examined the effects of PIM1-KD using siRNA on cellular functions in ARK1 cells. The WST-1 assay

FIG. 3. Effects of PIM1-KD by siRNA on cellular functions in ARK1 cells. (A) Results of the WST-1 assay. Cell proliferation/viability were significantly lower with PIM1-KD (PIM1-siRNA) than with the control ($P < 0.001$). (B) Photographs of control and PIM1-siRNA (PIM1-KD) and a graph of migration cell counts by the Transwell migration assay. PIM1-KD significantly reduced cell migration ($P < 0.001$). (C) Photographs of the control and PIM1-siRNA (PIM1-KD) and a graph of invasion cell counts by the Matrigel invasion assay. PIM1-KD significantly reduced cell invasion ($P < 0.001$).

revealed that cell viability was significantly lower in PIM1-KD cells than in the control (scrambled siRNA) (Fig. 3A). The transwell migration assay and matrigel invasion assay showed that PIM1-KD significantly decreased the number of migrating and invading cells (Figs. 3B, C). The PIM1 inhibitor, SGI-1776, down-regulated the expression of phospho-MYC, which is a downstream factor of PIM1 (Fig. 4A). Therefore, we investigated the effects of the PIM1 inhibitor (SGI-1776) on cell viability, migration, and invasion using SC cell lines. The WST-1 assay showed that SGI-1776 significantly reduced cell viability with IC50 between 1 and 5 μM in ARK1, ARK2, and SPAC2 and between 5 and 10 μM in SPAC1L (Fig. 4B). The transwell migration assay revealed that SGI-1776 significantly decreased migration at a concentration higher than 5 μM in ARK1 (Fig. 4C). Furthermore, the matrigel invasion assay revealed that SGI-1776 significantly inhibited invasion in ARK1 (Fig. 4D). Collectively, these results suggest the potential of PIM1 as a novel therapeutic target of SC.

Tumor Growth Suppression by the PIM1 Inhibitor

We conducted an *in vivo* study using ARK1 xenografts. Two weeks after the subcutaneous transplantation of ARK1 cells into nude mice, we confirmed the formation of xenograft tumors of ~100 mm^3. The oral administration of SGI-1776 solution (SGI-1776 group) or solvent only (control group) was initiated. The suppression of tumor growth was significantly stronger in mice administered SGI-1776 than in control mice ($P = 0.001$) (Figs. 5A–C). No significant differences were observed in body weight gain between the 2 groups during the treatment period (data not shown), and SGI-1776 was safely administered.

DISCUSSION

The present results demonstrated that the immuno-histochemical expression of PIM1 was significantly stronger in SC than in low-grade EC. The JAK/STAT pathway contributes to regulating the expression of PIM1 (10), and STAT1 and STAT3 have been shown
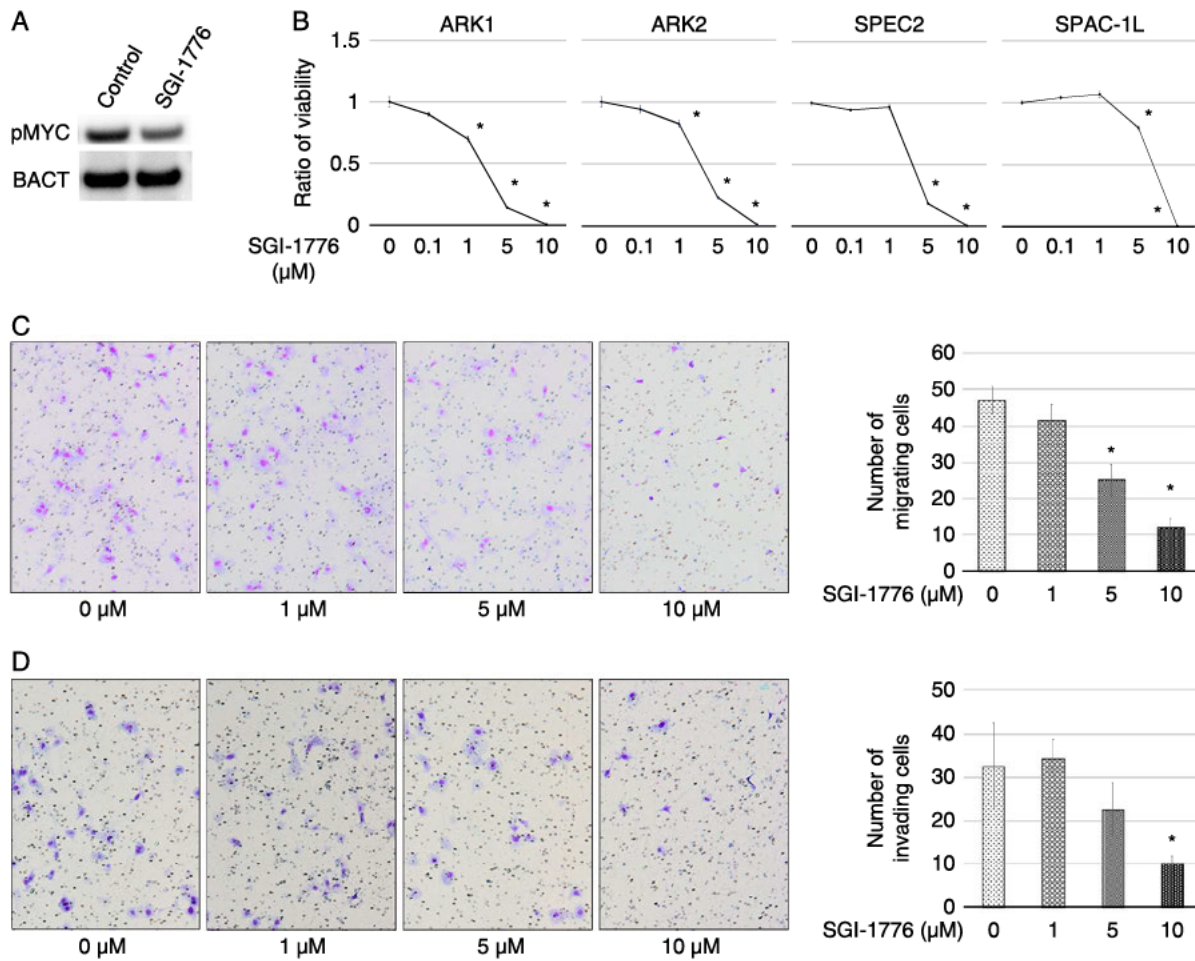
FIG. 4. Effects of the PIM1 inhibitor, SGI-1776, on cellular functions in serous carcinoma (SC) cell lines. (A) A treatment with SGI-1776 reduced the expression of phosphorylated MYC (pMYC), the target of PIM1, in ARK1 cells. (B–D) Effects of the SGI-1776 treatment on cellular functions in SC cells. (B) Results of the WST-1 assay. SGI-1776 dose-dependently reduced cell proliferation/viability in ARK1, ARK2, and SPAC2 with IC50 1 to 5 μM, and 5 to 10 μM in SPAC1L. Asterisks (*) indicate a significant difference from 0 μM ($P < 0.05$). (C) Photographs and a graph of the migration cell counts of ARK1 cells treated with each concentration of SGI-1776 by the Transwell migration assay. SGI-1776 dose-dependently reduced cell migration. Asterisks (*) indicate a significant difference from 0 μM ($P < 0.05$). (D) Photographs and a graph of the invasion cell counts of ARK1 cells treated with each concentration of SGI-1776 by the Matrigel invasion assay. SGI-1776 dose-dependently reduced cell invasion. Asterisk (*) indicate a significant difference from 0 μM ($P < 0.05$).

to enhance the JAK/STAT pathway in aggressive EMC, such as SC and high-grade EC (23). Furthermore, a relationship has been reported between the up-regulated expression of PIM1 and *PIM1* gene amplification in triple-negative breast cancer (24). As shown in TCGA data, the majority of SC cases are classified as the "Copy-number high" group based on a significantly high copy number variant frequency (15). This group consistently showed the *TP53* variant; however, the involvement of microsatellite instability or *PTEN* variants was rare. TCGA data also suggested that the 6p region, including the PIM1 gene locus (6p21.2), is frequently amplified in the "Copy-number high" group (25). In addition, we

confirmed the frequency of PIM1 gene amplification by TCGA data using cBioPortal (http://www.cbioportal.org/; last accessed on November 21, 2021) and revealed that PIM1 gene amplification was more frequent in USC (4%, 11/273 cases) than in EC (0.4%, 4/1095 cases). Median PIM1 mRNA expression was higher in cases with PIM1 amplification than in those with PIM1 diploid. Collectively, these results indicate that the JAK/STAT pathway and PIM1 gene amplification are involved in the overexpression of PIM1 in SC.

Protein phosphatase 2A (PP2A) is a phosphatase that exerts opposite effects to PIM1 kinase. It is a complex protein composed of a structural subunit A,
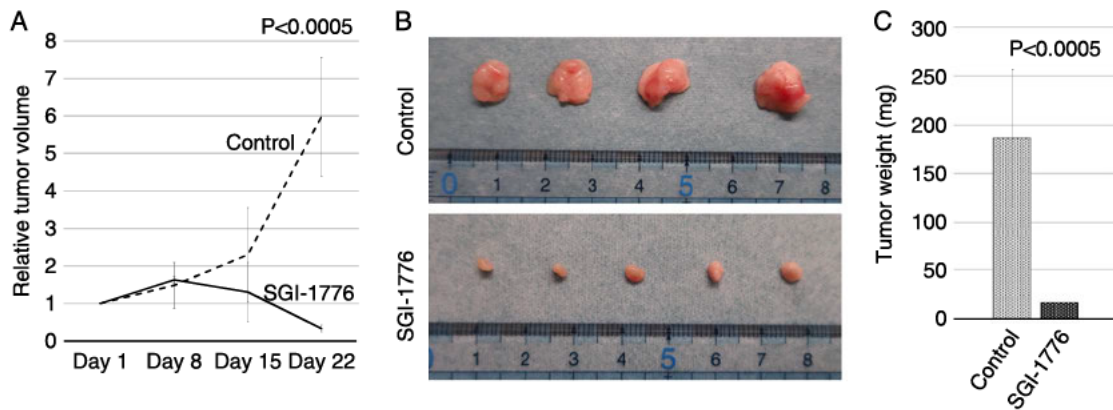
FIG. 5. Results of an *in vivo* study using ARK1 subcutaneous xenografts in nude mice. (A) Graph of relative tumor volumes on each treatment day. The SGI-1776 group was orally administered 75 mg/kg×5 times/wk of SGI-1776. The control group was only administered the solvent. The administration of SGI-1776 significantly suppressed tumor growth ($P < 0.0005$ on day 22). (B) Photographs of xenografts removed 3 wk after the initiation of oral administration. All xenografts were smaller in the SGI-1776 group than in the control group. (C) Graph of the tumor weight of removed xenografts in each group. Tumor weights were significantly smaller in the SGI-1776 group than in the control group ($P < 0.0005$).

such as PPP2R1A, a regulatory subunit B, and a catalytic subunit C. PP2A has been shown to degrade the PIM1 protein by dephosphorylation (26,27). The TCGA study demonstrated that the variant frequency of *PPP2R1A*, a component of PP2A, was high in the aggressive types: 22% in the "Copy-number high" group of EMC and 28% in cases of uterine carcinosarcoma(15,28); however, it was rare in the other groups of EMC. The PPP2R1A variant protein has been shown to impair the phosphatase activity of PP2A in a dominant-negative manner (29). The high frequency of the *PPP2R1A* variant in SC cases, most of which are in the "Copy-number high" group, may enhance the expression and functions of PIM1, resulting in increased malignancy.

The results of immunostaining demonstrated that PIM1 overexpression was rare in EIC, a precursor of SC, suggesting that it is not an early event in the development of SC. The overexpression of PIM1 was identified as an independent poor prognostic factor, which is consistent with the findings obtained for triple-negative breast cancer and clear-cell renal cancer (9,30). The limitation of the present study is the small number of cases at a single institution; however, TCGA data also reported the overexpression of *PIM1* mRNA was associated with a poor prognosis.

Our *in vitro* study revealed the involvement of PIM1 in the viability/proliferation of and migration and invasion by SC cells. These functions may directly contribute to increases in the malignant potential of tumor cells. The present results also suggested a role for PIM1 in the activation of MYC by phosphorylation. The topographical distribution of the immunohistochemical expression of PIM1 correlated with that of MYC. Wang et al. (31) reported that PIM1 activated MYC through the phosphorylation of serine-62 and synergistically enhanced prostate carcinogenesis. Brasó-Maristany et al. (9) also demonstrated that PIM1 functioned through the MYC activation pathway. In addition, TCGA data showed that the chromosome 8q region, including the *MYC* gene, was frequently amplified in the "Copy-number high" group (15,25). These findings are consistent with the present results and suggest that MYC is the most important substrate of PIM1. On the other hand, many other phosphorylation targets of PIM1 have been reported, including cell cycle regulatory proteins, such as Wee1, and apoptosis-related proteins (10,32). We examined the expression of BAD, a target apoptosis-related protein of PIM1; however, no changes in phosphorylation levels were induced by PIM1 siRNA or SGI-1776 (data not shown). Therefore, we were unable to clarify the involvement of PIM1 target factors other than MYC in SC.

Our *in vivo* results indicated that the administration of SGI-1776 suppressed ARK1 xenograft tumor growth. Several molecular targeted drugs are currently effective against EMC (2). The phosphatidylinositol-3 kinase (PI3K) pathway is activated in EMC by PTEN-inactivated or PIK3CA-activated mutations (15). However, two randomized control trials failed to show any beneficial effects of PI3K/AKT/mTOR inhibitors (33). HER2/ERBB2 overexpression and gene amplification

were detected in ~61% and 21% of USC cases, respectively (34). Fader et al. (3) reported the result of the phase II study in patients with advanced or recurrent USC that demonstrated an improvement in PFS (8 vs. 12.9 mo; hazard ratio, 0.46; $P = 0.005$) and overall survival (24.4 vs. 29.6 mo; hazard ratio, 0.58; $P = 0.046$) favoring the trastuzumab, a humanized anti-HER2 monoclonal antibody, with chemotherapy arm when compared with chemotherapy alone. These preliminary data are encouraging, and now trastuzumab is recommended by the National Comprehensive Cancer Network guidelines (Uterine Neoplasm Version2. 2021, last accessed on June 3, 2021 in https://www.nccn.org/guidelines/category_1). On the other hand, since the PI3K pathway is the main downstream pathway of HER2 signaling, its activation by a *PTEN* or *PIK3CA* mutation may be one of the mechanisms underlying the development of resistance to anti-HER2 therapy. Antibody drugs against the immune checkpoint molecule, PD-1, were previously shown to be moderately effective in EMC cases harboring microsatellite instability (35). However, SC cases are generally included in the "Copy-number high" group without microsatellite instability (21). Therefore, the anti-PD-1 antibody monotherapy may not be effective against SC. Recently, the effectiveness of the Wee1 inhibitor adavosertib in recurrent USC has been reported (6). Notably, Wee1, one of the cell cycle regulatory proteins, is reported as the phosphorylation target of PIM1 (36). These facts make more promising the effectiveness of PIM1 for USC. Some cases of SC may have a homologous recombination deficiency caused by a high frequency of copy-number variants, for which PARP inhibitors may be useful. Therefore, a phase 2 clinical trial on SC using the PARP inhibitor, Niraparib, is ongoing (https://clinicaltrials.gov/ct2/show/NCT04080284). Since the mechanisms underlying the anti-tumor effects of PIM1 inhibitors may differ from those of other molecular targeted therapeutics, we consider PIM1 inhibitors to be a novel and promising therapeutic approach.

In conclusion, the present study demonstrated that the expression of PIM1 was stronger in SC than in low-grade EC, and its overexpression was identified as an independent poor prognostic factor. PIM1 functions were involved in cell viability/proliferation, invasion, and migration, and the inhibition or KD of PIM1 suppressed these functions and xenograft tumor growth. These results indicate the potential of PIM1 as a novel prognostic biomarker and therapeutic target for EMC, particularly SC, as well as SGI-1776 as a molecular target drug. Further studies are needed to clarify the beneficial effects of PIM1 inhibitors for the treatment of SC.

REFERENCES

1. Berstein LM, Tchernobrovkina AE, Gamajunova VB, et al. Tumor estrogen content and clinico-morphological and endocrine features of endometrial cancer. *J Cancer Res Clin Oncol* 2003;129:245–9.
2. Ferriss JS, Erickson BK, Shih IM, et al. Uterine serous carcinoma: key advances and novel treatment approaches. *Int J Gynecol Cancer* 2021;31:1165–74.
3. Fader AN, Roque DM, Siegel E, et al. Randomized phase II trial of carboplatin–paclitaxel compared with carboplatin–paclitaxel–trastuzumab in advanced (stage III–IV) or recurrent uterine serous carcinomas that overexpress Her2/Neu (NCT01367002): updated overall survival analysis. *Clin Cancer Res* 2020;26:3928–35.
4. Simpkins F, Drake R, Escobar PF, et al. A phase II trial of paclitaxel, carboplatin, and bevacizumab in advanced and recurrent endometrial carcinoma (EMCA). *Gynecol Oncol* 2015;136:240–5.
5. Liu JF, Xiong N, Campos SM, et al. Phase II study of the WEE1 inhibitor adavosertib in recurrent uterine serous carcinoma. *J Clin Oncol* 2021;39:1531–9.
6. Motiwala T, Jacob ST. Role of protein tyrosine phosphatases in cancer. *Prog Nucleic Acid Res Mol Biol* 2006;81:297–329.
7. Zhang Y, Wang Z, Li X, et al. Pim kinase-dependent inhibition of c-Myc degradation. *Oncogene* 2008;27:4809–19.
8. Xu J, Li P, Chai J, et al. The clinicopathological and molecular features of sinusoidal large B-cell lymphoma. *Mod Pathol* 2020;■:■. https://doi.org/10.1038/s41379-020-00685-7.
9. Brasó-Maristany F, Filosto S, Catchpole S, et al. PIM1 kinase regulates cell death, tumor growth and chemotherapy response in triple-negative breast cancer. *Nat Med* 2016;22:1303–13.
10. Nawijn MC, Alendar A, Berns A. For better or for worse: the role of Pim oncogenes in tumorigenesis. *Nat Rev Cancer* 2011;11:23–34.
11. Kirschner A, Wang J, Van Der Meer R, et al. PIM kinase inhibitor AZD1208 for treatment of MYC-driven prostate cancer. *J Natl Cancer Inst* 2015;107:1–11.
12. Shannan B, Watters A, Chen Q, et al. PIM kinases as therapeutic targets against advanced melanoma. *Oncotarget* 2016;7:54897–912.
13. Cervantes-Gomez F, Stellrecht CM, Ayres ML, et al. PIM kinase inhibitor, AZD1208, inhibits protein translation and induces autophagy in primary chronic lymphocytic leukemia cells. *Oncotarget* 2019;10:2793–809.
14. Keeton EK, McEachern K, Dillman KS, et al. AZD1208, a potent and selective pan-Pim kinase inhibitor, demonstrates efficacy in preclinical models of acute myeloid leukemia. *Blood* 2014;123:905–13.
15. Getz G, Gabriel SB, Cibulskis K, et al. Integrated genomic characterization of endometrial carcinoma. *Nature* 2013;497:67–73.
16. Ida K, Yamanoi K, Asaka S, et al. αGlcNAc and its catalyst α4GnT are diagnostic and prognostic markers in uterine cervical tumor, gastric type. *Sci Rep* 2019;9:1–9.
17. Varughese J, Cocco E, Bellone S, et al. Uterine serous papillary carcinomas overexpress human trophoblast-cell-surface marker (trop-2) and are highly sensitive to immunotherapy with hRS7, a humanized anti-trop-2 monoclonal antibody. *Cancer* 2011;117:3163–72.

AQ1
AQ2

18. Hirai Y, Kawaguchi T, Hasumi K, et al. Establishment and characterization of human cell lines from a serous papillary adenocarcinoma of the endometrium. *Gynecol Oncol* 1994;54:184–95.

19. Boyd JA, Rinehart CA, Walton LA, et al. Ultrastructural characterization of two new human endometrial carcinoma cell lines and normal human endometrial epithelial cells cultured on extracellular matrix. *Vitr Cell Dev Biol* 1990;26:701–8.

20. Miyamoto T, Kashima H, Suzuki A, et al. Laser-captured microdissection-microarray analysis of the genes involved in endometrial carcinogenesis: stepwise up-regulation of lipocalin2 expression in normal and neoplastic endometria and its functional relevance. *Hum Pathol* 2011;42:1265–74.

21. Suzuki A, Horiuchi A, Ashida T, et al. Cyclin A2 confers cisplatin resistance to endometrial carcinoma cells via up-regulation of an Akt-binding protein, periplakin. *J Cell Mol Med* 2010;14:2305–17.

22. Mvunta DH, Miyamoto T, Asaka R, et al. SIRT1 regulates the chemoresistance and invasiveness of ovarian carcinoma cells. *Transl Oncol* 2017;10:621–31.

23. Kharma B, Baba T, Matsumura N, et al. STAT1 drives tumor progression in serous papillary endometrial cancer. *Cancer Res* 2014;74:6519–30.

24. Wein L, Loi S. Mechanisms of resistance of chemotherapy in early-stage triple negative breast cancer (TNBC). *Breast* 2017;34:S27–30.

25. Taylor AM, Shih J, Ha G, et al. Genomic and functional approaches to understanding cancer aneuploidy. n.d. https://doi.org/10.1016/j.ccell.2018.03.007.

26. Ma J, Arnold HK, Lilly MB, et al. Negative regulation of Pim-1 protein kinase levels by the B56β subunit of PP2A. *Oncogene* 2007;26:5145–53.

27. Losman JA, Chen XP, Vuong BQ, et al. Protein phosphatase 2A regulates the stability of Pim protein kinases. *J Biol Chem* 2003;278:4800–5.

28. Cherniack AD, Shen H, Walter V, et al. Integrated molecular characterization of uterine carcinosarcoma. *Cancer Cell* 2017;31:411–23.

29. Haesen D, Asbagh LA, Derua R, et al. Recurrent PPP2R1A mutations in uterine cancer act through a dominant-negative mechanism to promote malignant cell growth. *Cancer Res* 2016;76:5719–31.

30. Zhao B, Liu L, Mao J, et al. PIM1 mediates epithelial-mesenchymal transition by targeting Smads and c-Myc in the nucleus and potentiates clear-cell renal-cell carcinoma onco-genesis article. *Cell Death Dis* 2018;9:■. https://doi.org/10.1038/s41419-018-0348-9.

31. Wang J, Kim J, Roh M, et al. Pim1 kinase synergizes with c-MYC to induce advanced prostate carcinoma. *Oncogene* 2010;29:2477–87.

32. Santio NM, Koskinen PJ. PIM kinases: from survival factors to regulators of cell motility. *Int J Biochem Cell Biol* 2017;93:74–85.

33. Roncolato F, Lindemann K, Willson ML, et al. Pi3K/AKT/mTOR inhibitors for advanced or recurrent endometrial cancer. *Cochrane Database Syst Rev* 2019;2019https://doi.org/10.1002/14651858.CD012160.pub2.

34. Grushko TA, Filiaci VL, Mundt AJ, et al. An exploratory analysis of HER-2 amplification and overexpression in advanced endometrial carcinoma: a gynecologic oncology group study. *Gynecol Oncol* 2008;108:3–9.

35. Marabelle A, Le DT, Ascierto PA, et al. Efficacy of pembrolizumab in patients with noncolorectal high micro-satellite instability/ mismatch repair–deficient cancer: results from the phase II KEYNOTE-158 study. *J Clin Oncol* 2020;38:1–10.

36. Herzog S, Fink MA, Weitmann K, et al. Pim1 kinase is upregulated in glioblastoma multiforme and mediates tumor cell survival. *Neuro Oncol* 2015;17:223–42.